

2016

# Preliminary Analysis of a Fully Solid State Magnetocaloric Refrigeration

Mingkan Zhang

*Oak Ridge National Laboratory, United States of America, zhangm1@ornl.gov*

Ayyoub Mehdizadeh Momen

*Oak Ridge National Laboratory, United States of America, momena@ornl.gov*

Omar Abdelaziz

*Oak Ridge National Laboratory, United States of America, abdelazizoa@ornl.gov*

Follow this and additional works at: <http://docs.lib.purdue.edu/iracc>

---

Zhang, Mingkan; Mehdizadeh Momen, Ayyoub; and Abdelaziz, Omar, "Preliminary Analysis of a Fully Solid State Magnetocaloric Refrigeration" (2016). *International Refrigeration and Air Conditioning Conference*. Paper 1758.  
<http://docs.lib.purdue.edu/iracc/1758>

This document has been made available through Purdue e-Pubs, a service of the Purdue University Libraries. Please contact [epubs@purdue.edu](mailto:epubs@purdue.edu) for additional information.

Complete proceedings may be acquired in print and on CD-ROM directly from the Ray W. Herrick Laboratories at <https://engineering.purdue.edu/Herrick/Events/orderlit.html>

## Preliminary Analysis of a Fully Solid State Magnetocaloric Refrigeration

Mingkan Zhang<sup>1</sup>, Ayyoub Mehdizadeh Momen<sup>1</sup>, Omar Abdelaziz<sup>1\*</sup>

<sup>1</sup>Building Equipment Research, Oak Ridge National Laboratory  
Oak Ridge, TN, USA

Phone: 865-574-2089, Fax: 865-574-9338, Email: [abdelazizoa@ornl.gov](mailto:abdelazizoa@ornl.gov)

\* Corresponding Author

### ABSTRACT

Magnetocaloric refrigeration is an alternative refrigeration technology with significant potential energy savings compared to conventional vapor compression refrigeration technology. Most of the reported active magnetic regenerator (AMR) systems that operate based on the magnetocaloric effect use heat transfer fluid to exchange heat, which results in complicated mechanical subsystems and components such as rotating valves and hydraulic pumps. In this paper, we propose an alternative mechanism for heat transfer between the AMR and the heat source/sink. High-conductivity moving rods/sheets (e.g. copper, brass, iron, graphite, aluminum or composite structures from these) are utilized instead of heat transfer fluid significantly enhancing the heat transfer rate hence cooling/heating capacity. A one-dimensional model is developed to study the solid state AMR. In this model, the heat exchange between the solid-solid interfaces is modeled via a contact conductance, which depends on the interface apparent pressure, material hardness, thermal conductivity, surface roughness, surface slope between the interfaces, and material filled in the gap between the interfaces. Due to the tremendous impact of the heat exchange on the AMR cycle performance, a sensitivity analysis is conducted employing a response surface method, in which the apparent pressure, effective surface roughness and grease thermal conductivity are the uncertainty factors. COP and refrigeration capacity are presented as the response in the sensitivity analysis to reveal the important factors influencing the fully solid state AMR and optimize the solid state AMR efficiency. The performances of fully solid state AMR and traditional AMR are also compared and discussed in present work. The results of this study will provide general guidelines for designing high performance solid state AMR systems.

### 1. INTRODUCTION

The magnetocaloric refrigeration is based on the magnetocaloric effect (MCE), which induces an adiabatic temperature change of a magnetocaloric material (MCM) during the change of the magnetic field. However, it is well known that the MCE of most magnetocaloric materials at moderate magnetic fields (up to 1.5 T) is limited to a maximum adiabatic temperature change of 5 K, so such materials cannot be directly implemented into a practical cooling or heating device where temperature span over 30 K is required. The idea of AMR was introduced by Barclay and Steyert, 1982 to address this problem, in which a regenerative cycle is applied to create temperature spans high enough comparable to traditional cooling systems. From then on the AMR has become an interesting topic in magnetic refrigeration community for several decades, because it provides an alternative refrigeration technology with significant potential energy savings compared to conventional vapor compression refrigeration technology at room temperature. A large number of experimental and numerical studies have been documented AMR research. This can be illustrated in the review papers (Engelbrecht et al., 2011; Franco et al., 2012; Gschneidner and Pecharsky, 2008; Nielsen et al., 2011; Romero Gómez et al., 2013; B. Yu et al., 2003; Bingfeng Yu et al., 2010).

Although great improvements in AMR performance have been achieved and some prototype AMR devices have been developed, its commercialization has faced several challenges, e.g. the high cost due to the low system frequency, the need of a pump or rotating valve for fluidic system, and low heat transfer rate because of the low thermal conductivity of the fluids. One of the potential solutions recently proposed to address these challenges is the replacement of the heat exchange fluids by solid state materials. However, AMR has so far been restricted to applications using fluids and very little work has been reported about solid state AMR. To the best of our

knowledge, only Silva et al. and Silva et al. (Silva et al., 2012, 2014) published an ideal design of solid state AMR based on a new kind of material whose thermal conductivity changes with magnetic field as a gate to control the direction of heat exchange instead of direction of fluid flow. However, this design is highly dependent on the breakthrough in material science to provide such kind of new material. Alternatively, in present work, we propose a novel fully solid state AMR, in which high-conductivity moving rods/sheets (e.g. copper, brass, iron, graphite, aluminum or composite structures from these) are utilized instead of heat transfer fluid significantly enhancing the heat transfer rate, and hence cooling/heating capacity. The aim of present work is to illustrate the description, modeling and numerical simulation of the fully solid state AMR. The heat exchange between the solid-solid interfaces is modeled via a contact conductance, which depends on the interface apparent pressure, material hardness, thermal conductivity, surface roughness, surface slope between the interfaces and the thermal grease filled in the gap. Based on the model, a sensitivity analysis is performed by employing a response surface method, in which the uncertainty factors are the apparent pressure, effective surface roughness, and thermal grease thermal conductivity and responses are Cooling Capacity and COP. In additional, a performance comparison between solid state AMR and traditional AMR is conducted. The influences of utilization and frequency on the AMR performance are discussed in detail.

## 2. FULLY SOLID STATE ACTIVE MAGNETIC REGENERATOR

The proposed fully solid state AMR is based on the patent application filed by ORNL (Momen et al., 2014), which uses high conductivity moving sheets (copper in present work) to substitute fluids in traditional AMR designs for heat transfer. In the solid state AMR, the gap between the body of MCM and the moving sheet is full of low-viscosity thermal grease to lubricate the contact surface as well as to minimize the thermal resistance of the gap. The solid state AMR provides exceptional heat transfer characteristics, which cannot be achieved with a fluidic AMR system. Considering the thermal conductivity of copper (385 W/(m·K)) is more than 500 times as water (0.6 W/(m·K)) at 298 K (Hugh, 1992), the solid state AMR could offer a tremendous increase in heat transfer rate based on the solid state material compared to the fluidic AMR. On the other hand, the enhanced heat transfer rate and low friction between the moving sheet and the MCM body will allow a significant increase in the machine operating frequency, leading to a dramatic enhancement of cooling capacity. Moreover, the solid state AMR eliminates the need of a pump or rotating valve, which not only avoids significant parasitic losses due to the pump/valve, but also provides cost savings.

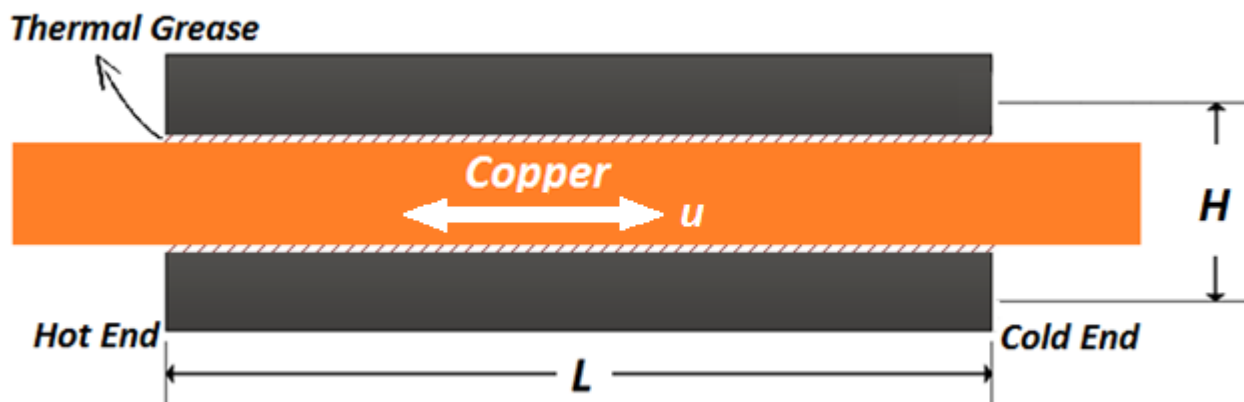


**Figure 1:** A schematic view of the solid state AMR.

Figure 1 shows a schematic view of the solid state AMR with moving sheet through the two “hot and cold” heat exchange spots, which consists of a solid state sheet with height  $\varepsilon H$  as the heat transfer material surrounded by the body of MCM. Similar to the fluidic AMR, the solid state AMR consists of following four processes, which can overlap in time: a) the AMR is magnetized and heats up due to the MCE; b) next, the high conductivity moving sheet move through the AMR and the MCM transmits the heat to the moving sheet; c) in the third step the AMR is demagnetized and its temperature decreases; d) finally, the solid sheet move in the counter-direction (relative to step two), the sheet are cooled down and the MCM in the AMR is heated up.

### 3. MATHEMATIC MODEL

A one-dimensional model has been developed for the AMR using solid state heat transfer material (e.g. copper), as described,

$$(h_c + h_g)a_c(T_s - T_r) + (1 - \varepsilon)k_r \frac{\partial^2 T_r}{\partial x^2} = (1 - \varepsilon)\rho_r T_r \left(\frac{\partial s}{\partial B}\right)_T \frac{\partial B}{\partial t} + (1 - \varepsilon)\rho_r c_B \frac{\partial T_r}{\partial t}, \quad (1)$$

$$-(h_c + h_g)a_c(T_s - T_r) + \varepsilon k_s \frac{\partial^2 T_s}{\partial x^2} = \varepsilon \rho_s c_s \frac{\partial T_s}{\partial t} + \varepsilon \rho_s c_s u \frac{\partial T_s}{\partial x}, \quad (2)$$

where  $a_c$ ,  $\varepsilon$ ,  $u$ ,  $s$ , and  $B$  are the contact area, porosity, velocity of solid state heat transfer material, entropy and applied magnetic field, respectively.  $T$ ,  $\rho$ ,  $k$ , and  $c$  represent temperature, density, thermal conductivity, and specific heat, respectively, in which subscripts  $r$  and  $s$  indicate regenerator and solid state heat transfer material, respectively.  $h_c$  is the contact conductance between refrigerant and solid state sheet, and can be written as (Negus and Yovanovich, 1988)

$$h_c = \frac{1.25\theta k_s}{\sigma} \left(\frac{P}{H_0}\right)^{0.95}, \quad (3)$$

where  $P$  is the apparent pressure on the interface and  $H_0$  is the hardness of the softer material.  $k_m$ ,  $\sigma$ , and  $\theta$  are the harmonic mean thermal conductivity, effective surface roughness, and effective absolute surface slope gap conductance, respectively, defined as

$$k_m = 2k_r k_s / (k_r + k_s), \quad (4)$$

$$\sigma = \sqrt{\sigma_r^2 + \sigma_b^2}, \quad (5)$$

$$\theta = \sqrt{\theta_r^2 + \theta_b^2}. \quad (6)$$

The gap conductance is

$$h_g = k_g / Y, \quad (7)$$

where  $k_g$  is the thermal conductivity of the gap substance. The effective gap thickness  $Y$  can be calculated by means of the simple power-law correlation equation proposed by Antonetti and Yovanovich (V. Antonetti and Yovanovich, 1984),

$$Y = 1.53\sigma \left(\frac{P}{H_0}\right)^{-0.097}. \quad (8)$$

Since the mean effective absolute surface slope and effective surface roughness are not independent, the correlation equation proposed by Antonetti et al. (Antonetti et al., 1993) was used in this case to calculate  $\theta$  from  $\sigma$ ,

$$\theta = 0.125(\sigma * 10^6)^{0.402}, \quad (9)$$

for the surface roughness range from 0.2  $\mu\text{m}$  to 9.6  $\mu\text{m}$ .

The boundary conditions are as follows:

$$T_s(x = 0) = T_H, \frac{\partial T_r}{\partial x}(x = 0) = 0, \quad (10)$$

for the cold flow and

$$T_s(x = L) = T_C, \frac{\partial T_r}{\partial x}(x = L) = 0, \quad (11)$$

for the hot flow. In the boundary conditions above,  $L$  is the length of the regenerator,  $T_H$  and  $T_C$  are the temperature of hot and cold ends, which are located at  $x = 0$  and  $x = L$ , respectively.

The equations are discretized on a uniform one-dimensional mesh and solved implicitly using a sparse matrix decomposition algorithm with the boundary conditions. A MATLAB code based on Engelbrecht (Engelbrecht, 2008) is developed to solve the time-dependent equations. The equations are solved by starting from a temperature distribution guess and stepping the model forward in time until steady state has been achieved. Then the steady state results are used to calculate cooling capacity, rejected heat and COP. The cooling capacity, rejected heat, COP, and utilization are calculated using the following equations,

$$\text{cooling capacity} = \frac{1}{\tau} \int_0^{\tau_{flow}} \dot{m} c_s (T_C - T_s(x = L)) dt, \quad (12)$$

$$\text{rejected heat} = \frac{1}{\tau} \int_0^{\tau_{flow}} \dot{m} c_s (T_s(x = 0) - T_H) dt, \quad (13)$$

$$\dot{W}_{mag} = (\text{Rejected Heat} - \text{Cooling Capacity}), \quad (14)$$

$$\text{COP} = \text{Cooling Capacity} / \dot{W}_{mag}, \quad (15)$$

$$U = \frac{\dot{m}_s \tau_{flow} c_s}{m_r c_r}. \quad (16)$$

In the equations above,  $\tau$  is the cycle time, which is the multiplicative inverse of frequency  $f$ .  $\tau_{flow}$  is the time for cold flow and hot flow, since they are identical in present work.

To verify our model, we compared the results of simulating an AMR made of Gd using water as the heat transfer fluid with published results from Petersen et al. (Petersen et al., 2008). The comparison in Figure 2 shows a good agreement between each other.

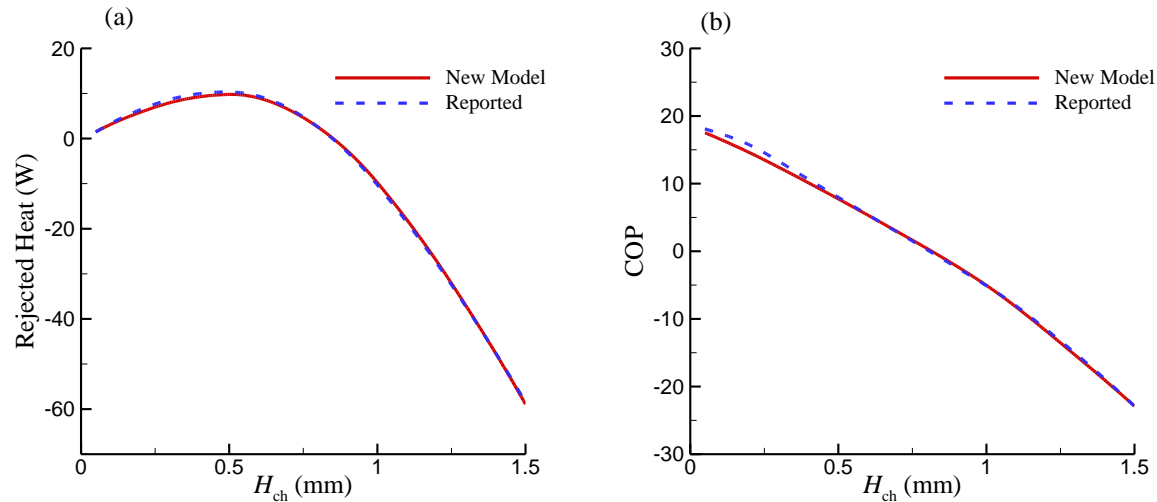


**Figure 2:** A comparison between numerical results from Petersen et al. [16] and present model on rejected heat and COP varying with channel height ( $H_{ch}$ ).

## 4. RESULTS AND DISCUSSIONS

The numerical simulations of solid state in this work are based on copper and Gd as the solid state heat transfer material and MCM, while for traditional AMR, nothing changes but substitute copper to water as the heat transfer material. The parameters used in present work are listed in the Table 1. Note that the physical properties of Gd depend on both the temperature and the magnetic field. The specific heat capacity and the specific entropy change of Gd used here are from Engelbrecht (Engelbrecht, 2008).

**Table 1:** Process parameters for the AMR cycle and material properties of different AMR materials.

Copper Density, $\rho_s$ (kg/m <sup>3</sup> )	8960
Copper Specific Heat, $c_s$ (J/(kg·K))	385
Copper Thermal Conductivity, $k_s$ (W/(m·K))	385
Gd Density, $\rho_r$ (kg/m <sup>3</sup> )	7900
Gd Specific Heat, $c_r$ (J/(kg·K))	See text
Gd Thermal Conductivity, $k_r$ (W/(m·K))	10.5
Water Specific Heat, $c_w$ (J/(kg·K))	4183
Water Thermal Conductivity, $k_w$ (W/(m·K))	0.595
Water Viscosity, $\mu$ (kg/(m·s))	0.000891
Channel Length, $L$ (mm)	50
Channel Height, $H$ (mm)	0.25
Channel Width, $W$ (mm)	10
Porosity, $\varepsilon$	0.5
Hot End Temperature, $T_H$ (K)	298
Cold End Temperature, $T_C$ (K)	288
Max Magnetic Field, $B$ (T)	1.0

### 4.1 Sensitive Analysis

Based on the numerical model built for the solid state AMR, a sensitive analysis is conducted in order to reveal the important factors influencing the solid state AMR. Three parameters, apparent pressure  $P$ , effective surface roughness  $\sigma$ , and thermal conductivity of grease  $k_g$ , are chosen as the uncertainty factors in the sensitive analysis,

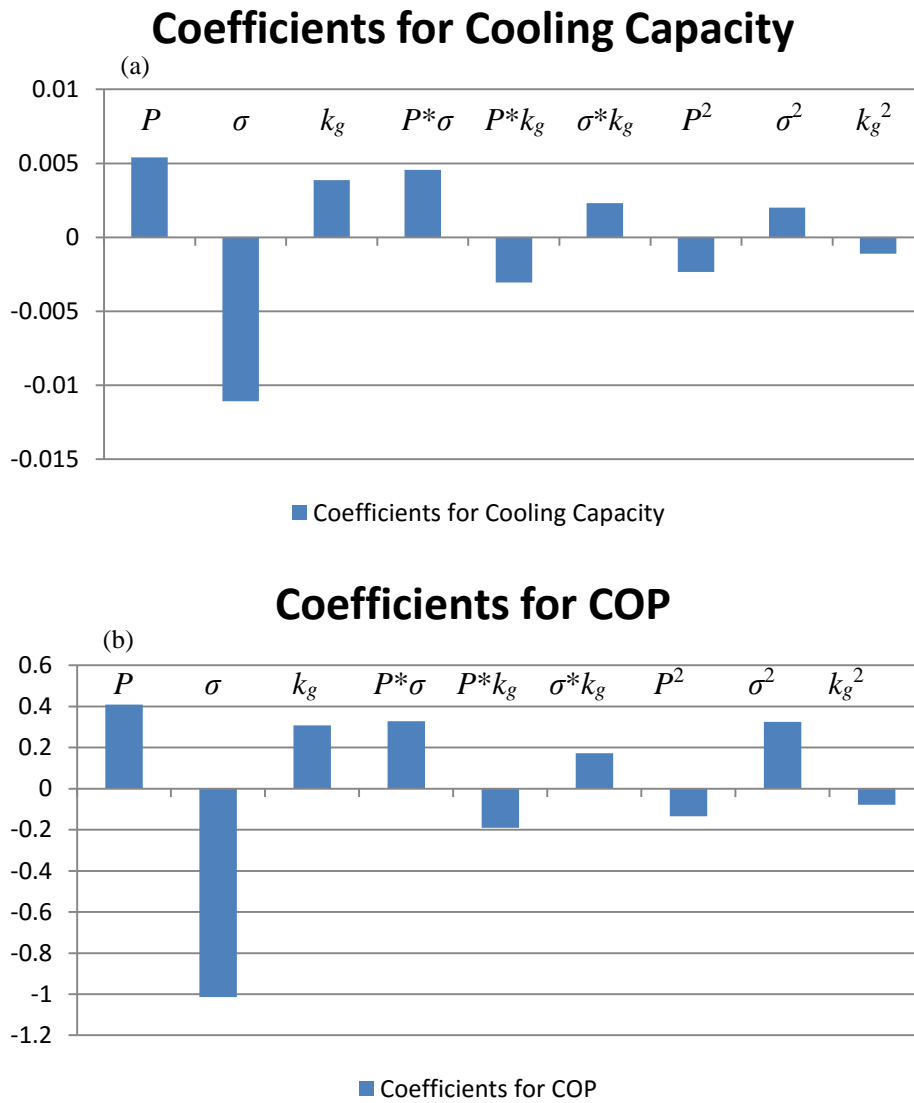
because they are unique for the cases of solid state AMR and controllable in experiments. The two most important results, Cooling Capacity and COP, are selected as the responses. A Box-Behnken Design (Box and Behnken, 1960) was employed to carry out the sensitive analysis in present work, in which three levels of each factor are tested as shown in Table 2. It aims to fit response surface models to the two responses as a function of the three controllable factors of the solid state AMR. Note that the runs 13 to 15 are repeated because in experimental studies, little differences are supposed to happen under the same experimental setup. However, for these numerical simulations, the results from them are exactly same.

**Table 2:** Runs of the Box-Behnken Design.

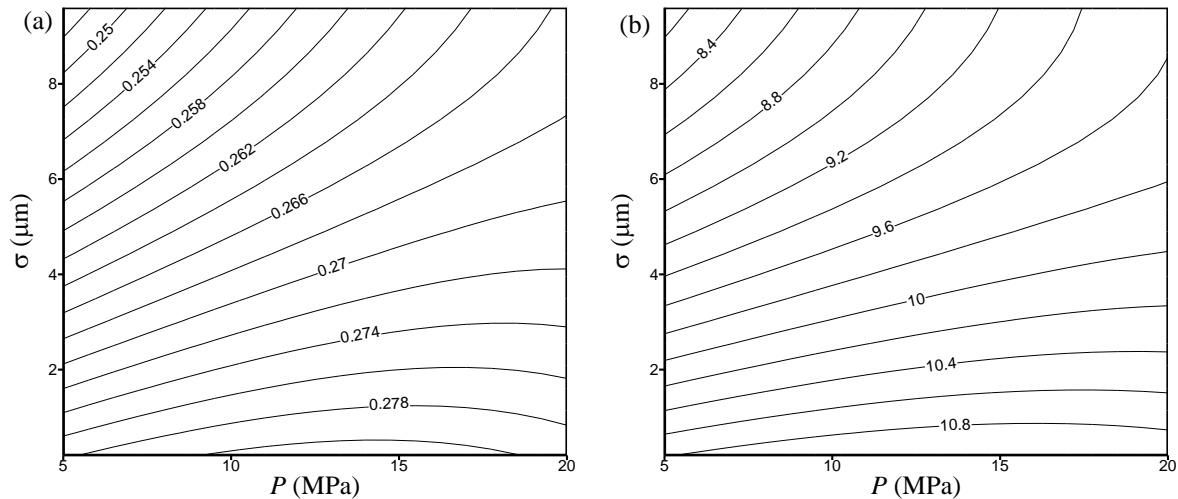
Run	Pressure (MPa)	Roughness ( $\mu\text{m}$ )	Conductivity ( $\text{W}/(\text{m}\cdot\text{K})$ )	Coded Pressure	Coded Roughness	Coded Conductivity
1	5	0.2	0.45	-1	-1	0
2	20	0.2	0.45	1	-1	0
3	5	9.6	0.45	-1	1	0
4	20	9.6	0.45	1	1	0
5	5	4.9	0.2	-1	0	-1
6	20	4.9	0.2	1	0	-1
7	5	4.9	0.7	-1	0	1
8	20	4.9	0.7	1	0	1
9	12.5	0.2	0.2	0	-1	-1
10	12.5	9.6	0.2	0	1	-1
11	12.5	0.2	0.7	0	-1	1
12	12.5	9.6	0.7	0	1	1
13	12.5	4.9	0.45	0	0	0
14	12.5	4.9	0.45	0	0	0
15	12.5	4.9	0.45	0	0	0

Figure 3 shows the coefficients of the fitting functions using coded factors in Table 1. It can be identified that the effective surface roughness contributes most to both COP and cooling capacity, while the apparent pressure makes the greater contribution than the thermal conductivity of grease. The sign of the coefficients represents that  $\sigma$  adversely affects the COP and Cooling Capacity and the rest two factors contribute positive impact on the responses. Since the Box-Behnken Design is a quadratic response surface model, the quadratic terms that indicate the non-linear behaviors and interactions between factors are also considered. For cooling capacity, the coefficient of  $P*\sigma$  is the greatest one among them, and even greater than the coefficient of  $k_g$ . For COP, however, the coefficients of both  $P*\sigma$  and  $\sigma^2$  are the two greatest ones. The great values of non-linear terms indicate that the response surface is not purely linear and non-linear terms also play a part in it.

Since Figure 3 suggests thermal conductivity of grease  $k_g$  is minor factor for COP and cooling capacity, the following sensitive analysis will focus on the effects of effective surface roughness  $\sigma$ , and apparent pressure  $P$  with a fixed  $k_g = 0.45 \text{ W}/(\text{m}\cdot\text{K})$ . Figure 4 depicts the contours of Cooling Capacity (a) and COP (b) as a function of  $\sigma$  and  $P$ . It can be identified from Figure 4 that  $P$  only influences COP and Cooling Capacity when the  $\sigma$  is high. For example, as shown in Figure 4 (a), when the  $\sigma$  is less than  $3 \mu\text{m}$ , the contour lines of Cooling Capacity and COP are almost parallel to the  $P$  axis, leading to weak effects of the  $P$  on the two responses. To provide a more straightforward visualization of the response surface, Figure 5 illustrates the 3D perspective plots of Cooling Capacity and COP. From Figure 5, it shows the little changes of COP and Cooling Capacity with  $P$  variation when the  $\sigma$  is small. In addition to  $P$ , as described above,  $\sigma$  plays the most important role among the three factors. Figure 5 reveals that with  $\sigma$  dropping, the Cooling Capacity and COP rapidly increase. After the  $\sigma$  reaches a small value, it dominates the changes of COP and cooling capacity. From the 3D plots, it can be found that the response surfaces for both COP and Cooling Capacity are not plates due to the non-linear effects. Therefore, from Figure 5, it can be concluded that the most efficient way to improve the COP and Cooling Capacity for the solid state AMR is to improve the smoothness for both solid state sheet and body of MCM. Especially, for the high Cooling Capacity and COP purposes, improvement of material smoothness seems the only way to further improve the two responses. From Figure 5, to optimize the output COP, larger  $P$  and smaller  $\sigma$  are demanded. Due to the non-linear effect, the sensitive analysis predicts that the optimization of Cooling Capacity occurs when  $P = 15 \text{ MPa}$  and  $\sigma = 0.2 \mu\text{m}$ .



**Figure 3:** Magnitudes of the Quadratic Model Coefficients for Cooling Capacity (a) and COP (b).



**Figure 4:** Contour plots of Cooling Capacity (a) and COP (b) with variances of  $P$  and  $\sigma$ .

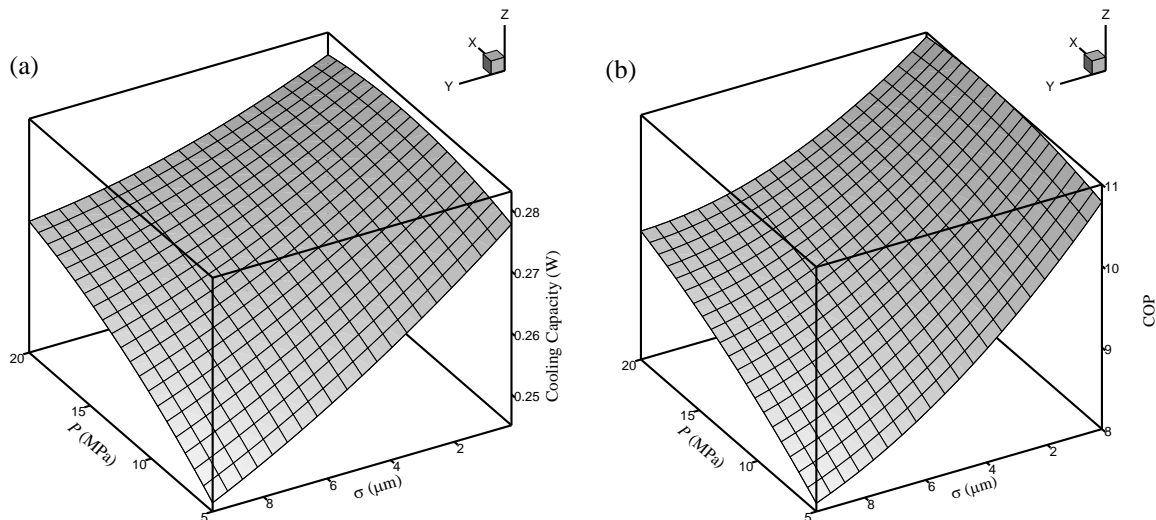


**Figure 5:** 3D perspective plots of COP (a) and Cooling Capacity (b) with variances of  $P$  and  $\sigma$ .

#### 4.2 Performance comparison between Solid State and traditional AMRs

The performances of solid state AMR and traditional AMR are also investigated in present work. Figure 6 illustrates a performance comparison between them, in which the apparent pressure  $P$ , effective surface roughness  $\sigma$ , and grease thermal conductivity  $k_g$  in solid state AMR are fixed at  $0.2 \mu\text{m}$ ,  $15 \text{ MPa}$  and  $0.7 \text{ W/(m}\cdot\text{K)}$ , respectively. For both water and copper as heat transfer material, the Cooling Capacity has different maximum values at different utilization, respectively. When the utilization is low, the heat transfer material moves so slowly that only a little Cooling Capacity can be produced. On the other hand, when the copper/water moves too quickly, the temperature profile of the AMR will be disturbed, resulting in a loss of cooling capacity (Li et al., 2006). Accordingly, there exists a utilization which provides the optimized Cooling Capacity. The numerical results show that the maximum Cooling Capacity increases linearly with frequency. It is because increasing the operation frequency not only increases the rate of copper/water motion but also increases the rate of magnetic work performed on the MCM. When the  $f = 0.5 \text{ Hz}$ , the traditional AMR provides a small positive Cooling Capacity with utilization from 0.2 to 2.4. Under the same frequency, the Cooling Capacity for solid state AMR is always negative with utilization changing, indicating that solid state AMR cannot work in the low operating frequency. When the frequency is raised ( $f = 5 \text{ Hz}$ ), the maximum Cooling Capacity of solid state AMR is about  $2.4 \text{ W}$ , which is much higher than the traditional AMR's maximum Cooling Capacity (about  $0.4 \text{ W}$ ) since the thermal conductivity of copper is much greater than that of water.



The COP variations with utilization when  $f = 0.5$  Hz and 5 Hz are depicted in Figure 6 (b). The COP of solid state AMR at  $f = 0.5$  Hz is not shown by Figure 6 (b) because it is always less than zero due to the negative cooling capacity at the same condition, Figure 6 (b) reveals that similar to the Cooling Capacity changing, there also exists a utilization which provides the optimized COP for a given frequency. However, with the frequency changing from 0.5 Hz and 5 Hz, the maximum COPs of solid state AMR and traditional AMR develops in different directions. When the frequency increases from 0.5 Hz and 5 Hz, the maximum COP of solid state AMR dramatically increases. Conversely, the maximum COP of traditional AMR decreases from 0.5 Hz and 5 Hz. It can be explained by the competition between Cooling Capacity and  $\dot{W}_{mag}$ , both of which increase with frequency increases. For solid state AMR, the Cooling Capacity increases more quickly than  $\dot{W}_{mag}$  when  $f$  is from 0.5 Hz and 5 Hz, leading to an enhanced maximum COP. However, the  $\dot{W}_{mag}$  increases faster than cooling capacity with the same frequency changing for the traditional AMR, so maximum COP decreases. Figure 6 (b) also represents that the maximum COP at  $f = 5$  Hz for solid state AMR is greater than the maximum COP at  $f = 0.5$  Hz for traditional AMR. Considering the discussion above that solid state provides a much higher Cooling Capacity when  $f = 5$  Hz, it can be concluded that at high frequency ( $f = 5$  Hz), the solid state AMR is capable of offering good COP and exceptional Cooling Capacity (approximately 8X improvement) simultaneously, which the traditional AMR cannot meet.

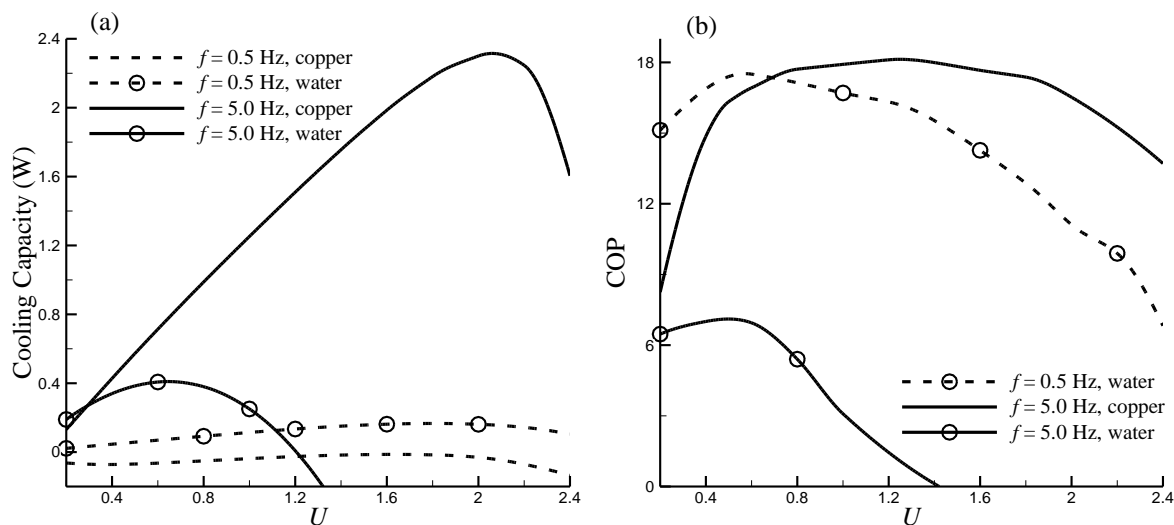


**Figure 6:** Cooling Capacity (a) and COP (b) as a function of utilization with  $f = 0.5$  and 5.0 Hz

## 5. CONCLUSIONS

A one dimensional model has been developed to study the solid state AMR, which combines the traditional AMR model as well as the heat transfer model between solid-solid with gap filled with thermal grease. The model was implemented to an AMR consisting of copper sheet as solid state heat transfer material and Gd sheets as MCM.

Based on the one dimensional solid state AMR model, a sensitive analysis was conducted to identify the important factors in the solid state AMR system. Three factors, apparent pressure  $P$ , effective surface roughness  $\sigma$ , and thermal conductivity of grease  $k_g$  were selected to test their influences on the two responses, Cooling Capacity and COP. The sensitive analysis results reveal that the effective surface roughness  $\sigma$  is the most impactful on Cooling Capacity and COP. In addition to the linear terms, non-linear terms also play a role in affecting Cooling Capacity and COP. The investigation indicates that improving the smoothness for both solid state sheet and body of MCM is the most efficient method to approach high Cooling Capacity and COP for the solid state AMR system.

The influence of utilization and frequency on Cooling Capacity and COP are also discussed. For both water and copper as heat transfer material, the cooling capacity/COP rises and then drops after reaching the maximum value with increasing utilization. It is also found that the maximum Cooling Capacity increases with frequency increasing, and the solid state AMR is able to provide an exceptional Cooling Capacity (approximately 8X improvement) than the traditional one when the frequency is high enough. For solid state AMR, the COP at 5 Hz was better than the best COP for traditional AMR. So it can be summarized that solid state AMR is able to offer a great Cooling

Capacity and COP simultaneously, which the traditional AMR cannot meet. Our numerical results show a great potential benefit to utilize solid state as a design of high performance AMR in the future.

## NOMENCLATURE

$a_c$	contact area	(m <sup>2</sup> )
$B$	applied magnetic field	(T)
$c$	specific heat	(J/kg·K)
$c_B$	specific heat at constant magnetic field	(J/kg·K)
$f$	frequency	(Hz)
$h$	conductance	(W/m <sup>2</sup> ·K)
$h_c$	contact conductance	(W/m <sup>2</sup> ·K)
$H$	channel height	(m)
$H_0$	hardness	(Pa)
$k$	thermal conductivity	(W/m·K)
$L$	channel length	(m)
$m$	mass	(kg)
$P$	apparent pressure	(Pa)
$s$	entropy	(J/kg·K)
$T$	temperature	(K)
$u$	velocity	(m/s)
$U$	utilization	(-)
$W$	channel width	(m)
$W_{mag}$	magnetic work	(J)
$Y$	effective gap thickness	(m)
$\varepsilon$	porosity	(-)
$\theta$	effective absolute surface slope	(°)
$\mu$	water viscosity	(kg/(m·s))
$\rho$	density	(kg/m <sup>3</sup> )
$\sigma$	surface roughness	(m)
$\tau$	cycle time	(s)
$\tau_{flow}$	time for cold flow and hot flow	(s)

### Subscript

C	cold end
m	harmonic mean
g	gap
H	hot end
r	regenerator
s	solid state heat transfer material

## REFERENCES

- Antonetti, V. W., Whittle, T. D., & Simons, R. E. (1993). An approximate thermal contact conductance correlation. *Journal of Electronic Packaging*, 115(1), 121–134.
- Antonetti, V. W., & Yovanovich, M. M. (1984). Thermal contact resistance in microelectronic equipment. *International Journal for Hybrid Microelectronics*.
- Barclay, J. A., & Steyert, W. A. (1982). Active magnetic regenerator.
- Box, G., & Behnken, D. (1960). Some new three level designs for the study of quantitative variables. *Technometrics*.
- Engelbrecht, K. (2008). *A numerical model of an active magnetic regenerator refrigerator with experimental validation*.
- Engelbrecht, K., Nellis, G., Klein, S., & Zimm, C. (2011). Review Article: Recent Developments in Room

- Temperature Active Magnetic Regenerative Refrigeration. *HVAC&R Research*, 13(4), 525–542.
- Franco, V., Blázquez, J., Ingale, B., & Conde, A. (2012). The Magnetocaloric Effect and Magnetic Refrigeration Near Room Temperature: Materials and Models. *Annual Review of Materials Research*, 42(1), 305–342.
- Gschneidner, K., & Pecharsky, V. (2008). Thirty years of near room temperature magnetic cooling: Where we are today and future prospects. *International Journal of Refrigeration*, 31(6), 945–961.
- Hugh D. (1992). *University Physics* (7th Edition). Addison Wesley.
- Li, P., Gong, M., Yao, G., & Wu, J. (2006). A practical model for analysis of active magnetic regenerative refrigerators for room temperature applications. *International Journal of Refrigeration*, 29(8), 1259–1266.
- Momen, A., Abdelaziz, O., & Vineyard, E. (2014). Magnetocaloric Refrigeration Using Solid Working Medium. US Provisional Patent Application, ID 3263.1.
- Negus, K., & Yovanovich, M. (1988). Correlation of the Gap Conductance Integral for Conforming Rough Surfaces. *Journal of Thermophysics and Heat Transfer*, 44–46.
- Nielsen, K. K., Tusek, J., Engelbrecht, K., Schopfer, S., Kitanovski, A., Bahl, C. R. H., Smith, A., Pryds, N., & Poredos, A. (2011). Review on numerical modeling of active magnetic regenerators for room temperature applications. *International Journal of Refrigeration*, 34(3), 603–616.
- Petersen, T., Engelbrecht, K., Bahl, C., Elmegaard, B., Pryds, N., & Smith, A. (2008). Comparison between a 1D and a 2D numerical model of an active magnetic regenerative refrigerator. *Journal of Physics D: Applied Physics*, 41(10), 105002.
- Romero Gómez, J., Ferreira Garcia, R., De Miguel Catoira, A., & Romero Gómez, M. (2013). Magnetocaloric effect: A review of the thermodynamic cycles in magnetic refrigeration. *Renewable and Sustainable Energy Reviews*, 17, 74–82.
- Silva, D., Bordalo, B., Pereira, A., Ventura, J., & Araújo, J. (2012). Solid state magnetic refrigerator. *Applied Energy*, 93, 570–574.
- Silva, D., Ventura, J., Araújo, J., & Pereira, A. (2014). Maximizing the temperature span of a solid state active magnetic regenerative refrigerator. *Applied Energy*, 113, 1149–1154.
- Yu, B., Gao, Q., Zhang, B., Meng, X., & Chen, Z. (2003). Review on research of room temperature magnetic refrigeration. *International Journal of Refrigeration*, 26(6), 622–636.
- Yu, B., Liu, M., Egolf, P., & Kitanovski, A. (2010). A review of magnetic refrigerator and heat pump prototypes built before the year 2010. *International Journal of Refrigeration*, 33(6), 1029–1060.

## ACKNOWLEDGEMENTS

This work was sponsored by the U. S. Department of Energy's Building Technologies Office under Contract No. DE-AC05-00OR22725 with UT-Battelle, LLC. We would like to acknowledge Mr. Antonio Bouza the Technology Manager for the HVAC & Appliances for his support.